

Design of LCoS-Based Twin 1 × 40 Wavelength Selective Switch



WANG Han^{1,2}, LIU Maoqi^{1,2}, FENG Zhenhua^{3,4},
LIU Minghuan^{3,4}, MAO Baiwei^{3,4}

(1. School of Optical and Electronic Information, Huazhong University of Science and Technology, Wuhan 430074, China;

2. Wuhan National Laboratory for Optoelectronics, Huazhong University of Science and Technology, Wuhan 430074, China;

3. WDM System Department of Wireline Product R&D Institute, ZTE Corporation, Wuhan 430223, China;

4. State Key Laboratory of Mobile Network and Mobile Multimedia Technology, Shenzhen 518055, China)

DOI: 10.12142/ZTECOM.202404004

<https://kns.cnki.net/kcms/detail/34.1294.TN.20241120.1118.002.html>,
published online November 20, 2024

Manuscript received: 2024-06-24

Abstract: Wavelength selective switch (WSS) is the crucial component in the reconfigurable optical add/drop multiplexer (ROADM), which plays a pivotal role in the next-generation all-optical networks. We present a compact architecture of twin 1×40 liquid crystal on silicon (LCoS)-based WSS, which can be regarded as a 4f system in the wavelength direction and a 2f system in the switching direction. It is designed with theoretical analysis and simulation investigation. Polarization multiplexing is employed for two sources of twin WSS by polarization conversion before the common optical path. The WSS system attains a coupling efficacy exceeding 96% for 90% of the ports through simulation optimization. The 3 dB bandwidth can be achieved by more than 44 GHz at a 50 GHz grid for all 120 channels at all deflection ports. This work establishes a solid foundation for developing high-performance WSS with larger port counts.

Keywords: wavelength selective switch (WSS); liquid crystal on silicon (LCoS); optical structure design; insertion loss

Citation (Format 1): WANG H, LIU M Q, FENG Z H, et al. Design of LCoS-based twin 1×40 wavelength selective switch [J]. *ZTE Communications*, 2024, 22(4): 18 – 28. DOI: 10.12142/ZTECOM.202404004

Citation (Format 2): H. Wang, M. Q. Liu, Z. H. Feng, et al., “Design of LCoS-based twin 1×40 wavelength selective switch,” *ZTE Communications*, vol. 22, no. 4, pp. 18 – 28, Dec. 2024. doi: 10.12142/ZTECOM.202404004.

1 Introduction

Reconfigurable optical add/drop multiplexer (ROADM) is essential for enhancing wavelength routing flexibility to meet the growing requirements of data traffic capacity in future elastic optical networks^[1–3]. Wavelength selective switches (WSSes) serve as essential components for dynamically manipulating optical signals in both the spectrum and space domains, significantly enhancing the agility and reliability of the network. There are several technologies used in the WSS system for beam steering, including liquid crystals (LC), microelectromechanical systems (MEMS), and liquid crystals on silicon (LCoS). Owing to its high spatial resolution, phase-only modulation, high port isolation, and flexible deployment capability of channel bandwidth, LCoS-based WSS provides performance benefits and is the current promising and economical solution^[3–5]. Various efforts have been implemented to improve its port count, operation bandwidth,

spectral granularity, and responding time^[6–8]. Meanwhile, its insertion loss (IL), polarization dependent loss (PDL) and crosstalk (XT) should also be promoted to harness the power budget of the optical link and increase its cascability^[9].

As to LCoS-based WSS, PDL comes from the polarization-dependent characteristic of LCoS. By employing the polarization diversity optics with half-wave plate (HWP) or quarter-wave plate (QWP), the light orthogonal to the modulation direction of LCoS can also be used to achieve polarization independence^[10]. The XT is mainly caused by the high-order diffractions of the steered light beam with the finite pixelated array, the limited phase quantization and the physical effects, such as fringing field effect, phase flicker, and device non-uniformity. Besides, the unwanted coupling can also be produced due to the inappropriate arrangement of output fibers^[11]. Different phase pattern design methods have been developed to minimize the phase deviation from the ideal blazed grating, such as simulated annealing^[12], Gerchberg-Saxton (GS) algorithm^[13–14], the genetic algorithm^[15], and hybrid algorithms^[10]. The above methods can define the output fiber posi-

This work was supported by ZTE Industry-University-Institute Cooperation Funds under Grant No. IA20230614004.

tion to achieve less unintentional coupling according to the obtained accurate position of the signal and other orders of diffractions^[7]. Meanwhile, the wavefront encoding phase pattern of the off-axis lens is suggested instead of a blazed grating for defocusing the high-order diffractions^[16]. The IL arises from the absorption and scattering of the optical components, the diffraction loss of LCoS, and the coupling loss from the fiber array misalignment and optical aberration. For a given structured system, the absorption loss is the fixed system loss unless the components with better performance are employed^[11]. The diffraction efficiency of LCoS can be promoted by Computer Generated Holography (CGH)^[11-15], wavefront encoding^[16], and phase compensation^[17].

Finisar developed the first programmable LCoS-based WSS with 50 GHz channel spacing, achieving a neighboring port isolation greater than 25 dB for 90 separate 50 GHz channels at -8 dB loss for polarized light^[6]. A 1×9-port LCoS-based WSS with multicasting ability was designed with an insertion loss of -7.6 dB and a crosstalk of -19.4 dB^[10]. To expand the switching capability, efforts are devoted to increasing the port's number of WSS. A stacked switch architecture of WSSes was proposed to realize 40 independent 1×12 WSSes with a single 4k LCoS device. It can be configured to support a 1×144 port wavelength routing, or a 12×12 wavelength cross-connect, with an insertion loss of around -4.58 dB on average^[8]. Commercially, Finisar has developed a 1×20 port programmable LCoS-based WSS supporting a bandwidth of 6 THz and a bandwidth resolution of 6.25 GHz^[18]. From the perspective of practical applications, broadening the spectrum, minimizing the design footprint and increasing integration are crucial for advancing WSS technology. Recently, 20-dimensional WSS devices have been widely deployed in the current ROADM network^[19], and there is an increasing demand for WSS devices that offer higher dimensionality and integration. Higher-dimensional WSS requires larger deflection angles from the LCoS, demanding higher diffraction efficiency, especially in small-period grating set-up. Furthermore, the risk of crosstalk between channels increases with the number of ports, therefore novel isolation strategies and optimized optical paths are required to maintain the integrity of the optical signal. Precise alignment and advanced optical design are required to maintain high optical coupling efficiency with increased port numbers.

This work introduces an innovative theoretical method for designing optical paths in LCoS-based compact twin 1×40 WSS systems to meet commercial requirements. Our design stands out from existing commercial devices, which typically offer a maximum of 32 ports. The innovative twin structure significantly enhances integration, enabling the efficient accommodation of a larger number of ports. At the same time, it maintains performance metrics, such as insertion loss, crosstalk, and bandwidth, within commercial standards. A polarization diversity scheme and a polarization conversion system are

employed to facilitate efficient manipulation and control of polarization. Additionally, bending fiber arrays and a prism grating are designed to reduce conic diffraction and improve the coupling efficiency of the WSS. Computational simulations validate the design, achieving a coupling efficiency of 96% for 34 ports and over 80% for other ports. The 3 dB bandwidth meets commercial standards, reaching ≥ 44 GHz at a 50 GHz grid for all channels.

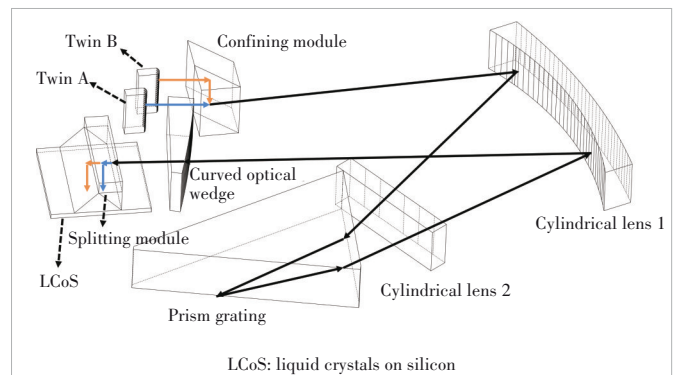
2 Optical Design of Twin WSS

2.1 Optical Architecture

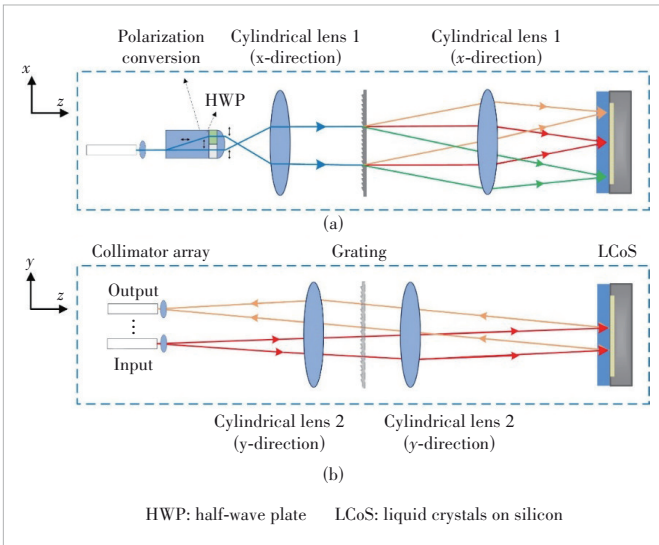
In developing commercial WSS, we aim to enhance port numbers, expand bandwidth, and integrate systems without compromising performance. To address the constraints of compactness and performance, we design a twin 1×40 WSS optical system as shown in Fig. 1. This system includes a fiber array and microlens array, a polarization conversion unit, cylindrical lens 1 and 2, a curved optical wedge, a confining module, and a splitting module before LCoS. The microlens array must be designed carefully to ensure that the returned light beam is coupled to the fiber array. In the polarization unit, the birefringent crystal and half-wave plate are used to manipulate the polarization states of light beams A and B for system multiplexing. The beam combiner before cylindrical lens 1 and the beam-splitting apparatus before LCoS aggregate and separate the light beams from twins A and B, respectively, leading to the zoning of the twin WSS on the LCoS. The prism grating is responsible for demultiplexing the wavelengths with high dispersion ability.

Fig. 2 shows the optical paths of WSS in the dispersion and switching directions. The WSS system employs a 4f configuration in the dispersion direction and a 2f configuration in the switching direction. In the dispersion direction, the signal light beam, after polarization modulation, is collimated by a cylindrical lens, then wavelength-demultiplexed by a prism grating, and reflected again by cylindrical lens 1, forming a 4f system. The dispersed light is imaged onto the LCoS device, creating a dispersed spectrum distribution along the y -axis.

The light beams from twins A and B are directed at the up-



▲ Figure 1. Twin WSS architecture

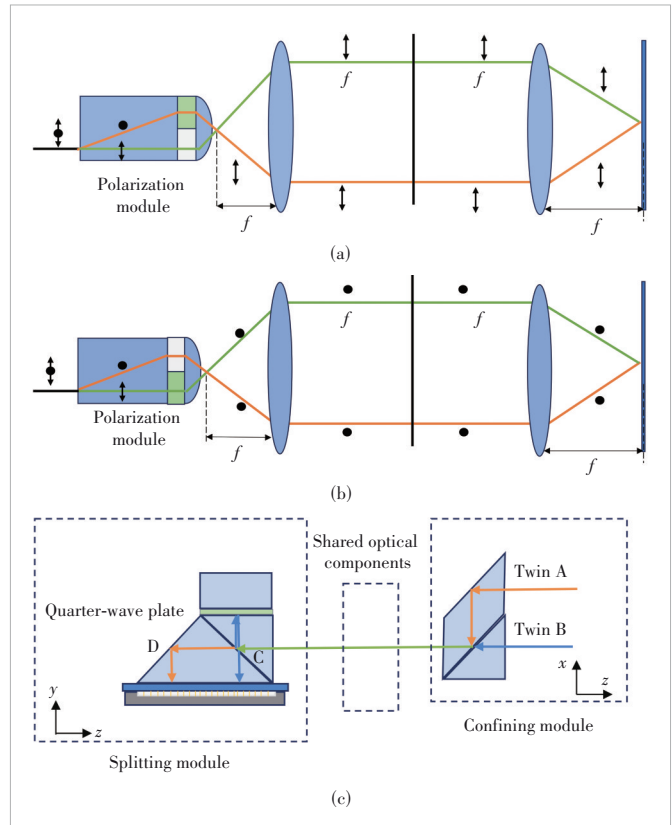


▲ Figure 2. Optical paths of WSS in (a) the dispersion direction and (b) the switching direction

per and lower halves of the LCoS, respectively. In the switching direction, cylindrical lens 2 and the LCoS constitute a $2f$ system. The dispersed light is imaged onto the LCoS, forming a rectangular dispersion spectrum within its active region. Phase grating holograms with various periods are imposed on the corresponding wavelength channels on the LCoS, facilitating the directional encoding of the light beams. The diffracted light from the LCoS emerges as the deflected collimation light corresponding to different output ports, which are focused by the micro-lens array onto the corresponding output ports, enabling low-loss optical switching between input and output ports for the given wavelength signal.

2.2 Twin WSS Structure Design

The LCoS utilized for our design has a resolution of 1920×1200 with a pixel pitch of $8 \mu\text{m}$, resulting in a length of 15.36 mm and 9.60 mm in the dispersion and switching directions, respectively. To minimize cross-talk between channel A and channel B of the twin WSS, the beam spot size of 3ω in the y -direction on the LCoS is set to smaller than 4.8 mm , which is half the width of the LCoS. Additionally, a factor of 0.9 is applied, resulting in a requirement that 3ω diameter should be less than 4.32 mm . Considering device and assembly tolerances, over 99.99% of the optical energy remains within half the LCoS width, effectively isolating the control regions of the two twin devices. A polarization diversity scheme is proposed to improve beam utilization efficiency and provide the possibility of dual source WSS with twin A and twin B. The key component of the scheme is a set of polarization modules, including birefringent crystals, half-wave plates (represented by the green rectangular in Fig. 3), and silicon-based micro-cylindrical lenses. The beam emitting from the micro-lens array can be modulated by adjusting the position of birefringent



▲ Figure 3. Schematic illustration of symmetric polarization loops established in the WSS: (a) polarization diversity of source A; (b) polarization diversity of source B; (c) polarization multiplexing in the twin WSS

crystals and half-wave plates to P-polarized light (Fig. 3a) and S-polarized light (Fig. 3b). The cylindrical lens leads the two polarization components to spatially coincide in the receiving plane while compressing the waist of the Gaussian beam in the dispersion direction.

To multiplex the optical elements for the beam signals from different sources, a polarization conversion system is proposed with a confining module and a splitting module, as shown in Fig. 3c. In the figure, the blue line represents the S-polarization state of the light from twin A and the orange line represents the P-polarization state of the light from twin B. The confining module combines light with two polarization states and ensures that light from both sources follows the same transmission path in the WSS system. As the LCoS is polarization-dependent, the polarization components are preferably rotated into alignment with the polarization axis of the LCoS. The splitting module, strategically positioned adjacent to the LCoS in the receiving plane, separates different sources of beams and unifies their polarization states. This module can be exactly modulated by the LCoS. Light from twin A passes through the polarizing interface C and is reflected by surface D to the upper half of the LCoS. Conversely, light from twin B is reflected by interface C, and undergoes polarization

rotation via an overhead quarter-waveplate twice. Subsequently, the light is incident on the lower half of the LCoS, and the polarization component is converted to the same as the light from twin A, which can be accurately manipulated by the LCoS.

3 Design of Twin 1×40 WSS with Performance Restriction Analysis

3.1 Wavelength Range

The designed WSS covers the super C band from 1 524 nm to 1 572 nm, approximately corresponding to frequencies from 190.637 5 THz to 196.675 THz, with a total bandwidth of approximately 6 THz. To optimize LCoS utilization, it is assumed that this bandwidth completely occupies the LCoS. In addition, the prism grating is meticulously crafted to achieve a superior level of spectral resolution. The schematic diagram of the prism grating is shown in Fig. 4a with a top angle of δ , a grating constant of d , a blazing angle of δ , a prism medium refractive index of n_A , and a glue layer refractive index of n_B .

We preliminarily design a prism grating with 1 500 lines/mm and a wedge angle of 77.52° to satisfy the operation frequency band from 190.637 5 THz to 196.675 THz. As light passes through the prism grating, different wavelengths diverge at various angles due to the prism refraction and grating diffraction. Utilizing the grating equation and an incidence angle of 52° , the exit angles for the central, minimum, and maximum wavelength are calculated. After reflecting from the grating, the beam exhibits an angular dispersion of $4.299 6^\circ$. This dispersion angle is further magnified after passing through the prism, resulting in a final exit angular dispersion of $8.969 8^\circ$ from the prism grating.

The coverage area of the beam on the LCoS is determined by the focal length of cylindrical lens 1 and the angular dispersion of prism grating, which can be described as

$$2f_{\text{lens}\#1} \tan\left(\frac{\theta(\lambda_{\text{max}}) - \theta(\lambda_{\text{min}})}{2}\right) = L_{\text{LCoS}}. \quad (1)$$

Taking into account the size L_{LCoS} of the LCoS in the dispersion direction and the angular dispersion of prism grating $\Delta\theta = \theta(\lambda_{\text{max}}) - \theta(\lambda_{\text{min}})$, cylindrical lens 1 with a focal length of 90 mm is selected to ensure a sufficient wavelength range.

3.2 Bandwidth Tuning Accuracy

The light beam is dispersed by the prism grating with different diffraction angles for different wavelengths. Subsequently, the dispersed light is focused by the imaging lens before the LCoS. From the imaging relation of the focus lens, the position of wavelength λ along the dispersion direction $x(\lambda)$ on the LCoS can be expressed as

$$x(\lambda) = f_{\text{lens}\#1} \tan[\theta_{\text{out}}(\lambda) - \theta_{\text{out}}(\lambda_0)], \quad (2)$$

where the diffraction angles of the incident light at wavelength λ and 1 548 nm are denoted by $\theta_{\text{out}}(\lambda)$ and $\theta_{\text{out}}(\lambda_0)$, respectively.

From the diffraction equation, the diffraction angle $\theta_{\text{out}}(\lambda)$ can be obtained from

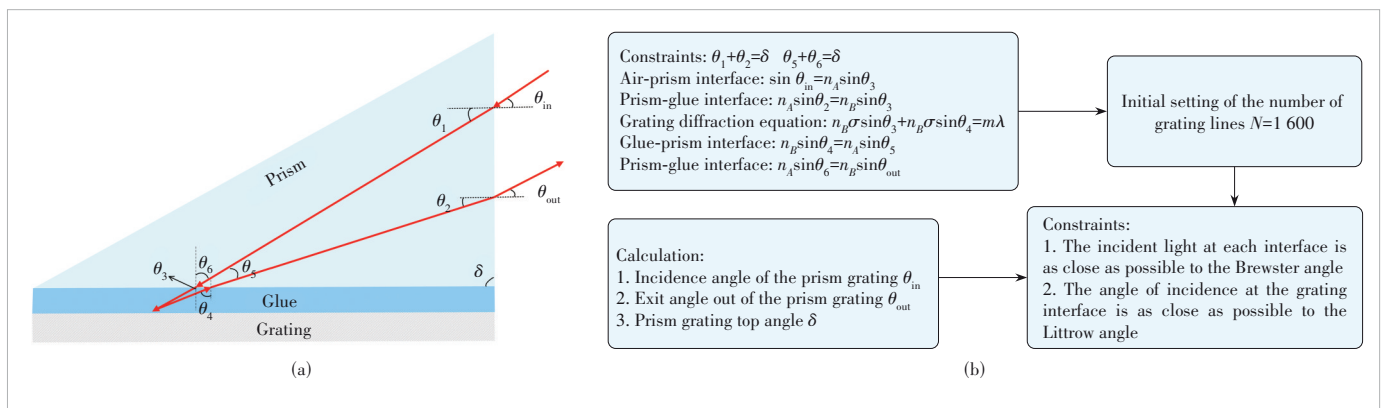
$$\sin\left[\sin^{-1}\left(\frac{\sin\theta_{\text{out}}(\lambda)}{n(\lambda)}\right) - \delta\right] - \sin\left[\sin^{-1}\left(\frac{\sin\theta_{\text{in}}}{n(\lambda)}\right) - \delta\right] = \frac{m\lambda}{n(\lambda)d}, \quad (3)$$

where $n(\lambda)$ can be calculated with the dispersion formula of prism material, m is the diffraction order, and d is the grating constant.

Assuming that the pixel pitch of the LCoS is d_{LCoS} , the spectral tuning accuracy R can be defined as the optical signal bandwidth corresponding to a change of one pixel on the LCoS, which can be expressed as

$$R = d_{\text{LCoS}} \frac{\partial\lambda}{\partial x}. \quad (4)$$

The smaller the spot size in the horizontal direction on the



▲ Figure 4. Schematic diagram of (a) prism grating and (b) its design process

LCoS, the sharper the spectral roll-off curve can be achieved. This enhances bandwidth characteristics.

Meanwhile, for the spectral resolution of a grating-based module, the finite width of the entrance slit should be taken into account rather than solely focusing on the diffraction limitation of the grating aperture. The minimum wavelength interval $(\Delta\lambda)_{\min}$ of two spectral components that are just resolvable according to the Rayleigh criterion can be described as

$$(\Delta\lambda)_{\min} \geq \left(\frac{\lambda}{a} + M \frac{b}{f_{\text{lens}\#1}} \right) \left(\frac{\partial\theta}{\partial\lambda} \right)^{-1}, \quad (5)$$

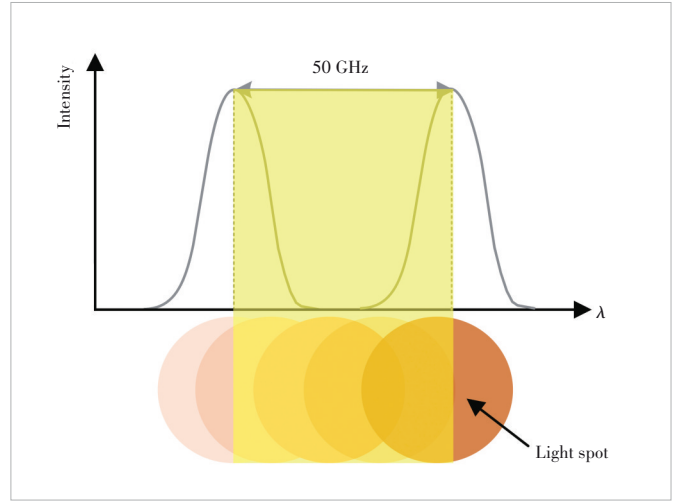
where λ is the operation wavelength, a is the system aperture determined by the aperture stop, b is the width of the entrance slit, $f_{\text{lens}\#1}$ is the focal length of the collimator lens between the entrance slit and the grating, and $\partial\theta/\partial\lambda$ represents the angular dispersion of the grating.

To meet the requirements for bandwidth tuning accuracy and minimum spectral resolution, we choose an LCoS pixel size of 8 μm and a focal length of 90 mm of lens#1. As a result, a bandwidth tuning accuracy of 6.25 GHz is achieved with a grating dispersion capability exceeding 0.002 $\text{rad}\cdot\text{nm}^{-1}$.

3.3.3 dB Bandwidth

Due to the wavelength continuity of the optical signal, the light spot will be overlapped in the margin of two neighbor channels, leading to the bandwidth for a grid channel smaller than the ideal bandwidth. The light spot size should be minimized to achieve better operational bandwidth performance. Given that the system is configured as a symmetric 4f, the Gaussian light spot on the LCoS surface aligns with that at the front focus of cylindrical lens 1. Thus, the waist of the light spot at the front focus of the cylindrical lens 1 must be carefully regulated using the micro-lens array and the lens positioned after the birefringent crystal. The system's bandwidth performance is evaluated by calculating the Gaussian beam waist required for the 3 dB and 0.5 dB bandwidths, as shown in Fig. 5.

Based on the equation of coupling efficiency between the optical fiber and the light spot, the fiber coupling efficiency is calculated for various ratios of the light spot being deflected to the desired direction. Fig. 6 illustrates the relations between the truncated position of the light spot and the coupling efficiency back into the fiber. To simulate an actual bandwidth testing scenario of an LCoS-WSS, we select a 50 GHz at a 6 dB window on the LCoS for the operation and calculate the 3 dB and 0.5 dB bandwidths. Assuming that the frequency range from 190.6375 THz to 196.675 THz corresponds to the 1920 pixels arranged horizontally on the LCoS, the 50 GHz grid channel occupies an average of 16 pixels. According to the results shown in Fig. 6, the following inequality must be satisfied to meet the WSS requirements^[20]:

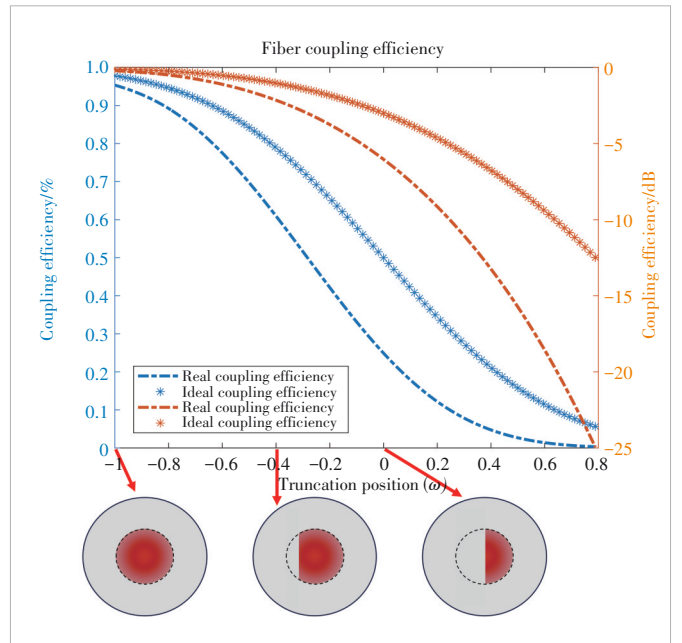


▲ Figure 5. Schematic diagram of the system's bandwidth

$$\begin{aligned} 50 \text{ GHz} \times (1 - 2 \times 0.283 \omega_{\text{LCoS}}/d) &> 46.0 \text{ GHz (3 dB)} \\ 50 \text{ GHz} \times (1 - 2 \times 0.798 \omega_{\text{LCoS}}/d) &> 37.5 \text{ GHz (0.5 dB)}, \quad (6) \end{aligned}$$

where ω_{LCoS} is the beam waist on the LCoS, and d is the window width on the LCoS.

Our analysis indicates that the ratio ω_{LCoS}/d should be less than 0.14. Assuming an average value for the windowing operation, each 50 GHz channel on the LCoS is allocated with a window of 128 μm , which implies that ω_{LCoS} is less than 18 μm . It is also important to note that the light spot is distributed non-uniformly along the horizontal direction on the LCoS for different wavelengths. With Zemax simulation results, the window widths of the 50 GHz channels should be set at 117 μm , 124 μm , and



▲ Figure 6. Fiber coupling efficiency for different truncation ratios

134 μm of the LCoS for the wavelengths of 1 524 nm, 1 548 nm, and 1 572 nm, respectively. This leads to the maximum beam waists of 16.53 μm , 17.52 μm , and 18.93 μm . Considering these factors comprehensively, the beam waist on the LCoS surface should be designed as $\omega_{\text{LCoS}} \leq 16 \mu\text{m}$, resulting in a 3 dB bandwidth of 46 GHz and a 0.5 dB bandwidth of 37.5 GHz.

3.4 Port Isolation

The isolation (ISO) can be represented as

$$\text{ISO} = 10 \times \log_{10} \left(\exp \left(-\frac{2a^2}{\omega^2} \right) \right), \quad (7)$$

where a is the spacing of the fiber array, and ω is the beam size at the front focal plane of the micro-lens.

It assumes all light not directed at the target fiber contributes to crosstalk, whereas, in reality, only a small fan-shaped region leaks into adjacent ports. This suggests that the calculation results of Eq. (7) are much more stringent for design.

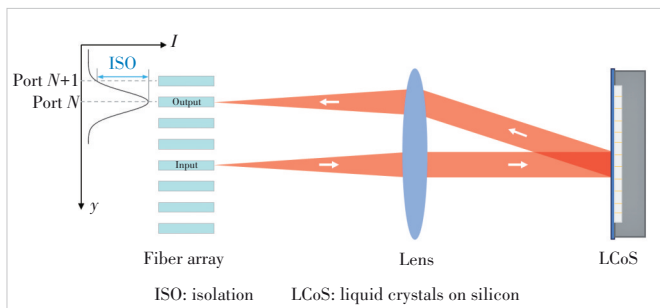
The port isolation of a WSS is primarily determined by the beam waist radius and the spacing of the fiber array (Fig. 7). Due to the limitation of steering efficiency, the period of the blazed grating displayed on the LCoS must exceed seven pixels. Consequently, the maximum steering angle is less than 1.38 degrees for a pixel size of 8 μm and less than 3.39 degrees for a pixel size of 3.74 μm . Increasing the spacing between fibers will inevitably reduce the number of available ports unless port isolation is compromised. For the given ISO of 25 dB, a fiber array of 40 ports with a spacing of 250 μm and a micro-lens array with a focal length of 0.73 μm are used.

3.5 Insertion Loss

Regarding the entire system structure, the insertion loss can be characterized as encompassing the prism grating loss, optical component absorption loss, LCoS diffraction loss, and fiber coupling, among other factors.

$$\text{IL} = \text{IL}_{\text{GRISM}} + \text{IL}_{\text{LCoS}} + \text{IL}_{\text{absorb}} + \text{IL}_{\text{coupling}} + \text{IL}_{\text{other}}. \quad (8)$$

Table 1 presents a theoretical analysis of the intrinsic insertion loss of the WSS. Generally, the difference between the experimental and theoretical values is small and could be attrib-



▲ Figure 7. Port isolation of a WSS system

▼ Table 1. Intrinsic loss of WSS

Component	Transmission	Pass	Loss/dB
Grism	0.87	2	-1.21
Intrinsic LCoS reflectivity	0.87	1	-0.60
System absorption	0.85	2	-1.42
Fiber coupling	0.85	1	-0.71
Total			-3.94

LCoS: liquid crystals on silicon WSS: wavelength selective switch

uted to the misalignment of the system and the diffraction efficiency of the LCoS. Particularly, the system adopts a polarization-insensitive prism grating, which has approximately the same diffraction efficiency for beams with different polarization states. The PDL can be controlled within 0.2 dB.

4 Simulation Performance Analysis

4.1 System Modeling Construction and Parameter Optimization

In our design, we have developed a microlens fiber array, polarization multiplexing module, beam combining module, cylindrical lens prism grating, and optical wedge with the entire system dimensioning approximately 110 mm × 90 mm × 15 mm. The simulation involves modeling a micro-lens array with a spacing of 250 μm and setting the input spectral range to 6 THz (between 1 524 nm and 1 572 nm). The central wavelength is set at 1 548 nm, with equal weighting given to the marginal wavelengths of 1 524 nm and 1 572 nm. The aperture value of the Gaussian beams is set to 5.2 μm . Additionally, the simulation included the emulation of a fiber optic array on the diaphragm surface, with the micro-lens array positioned after the diaphragm. In the system simulation, the micro-lens acts as a single lens with a radius of curvature of 1.849 mm and a thickness of 2.57 mm. It enlarges the size of the incoming Gaussian beam waist to 69 μm . Behind the micro-lens, a collection of Fourier lenses is positioned, with a combined focal length of 150 mm prior to optimization. Simultaneously, the micro-lens array is put in the front focal plane of lens#1, which causes the beam to become collimated and form parallel light. Once the lens group focuses the beam into parallel light by the lens group, it reaches the prism grating positioned on its back focal plane. The distance between the grating and lens#1 is typically no more than 90 mm, which ensures that the collimated light emitted from the Fourier lens group experiences minimal loss and reduces the overall size of the system. Then the prism grating disperses the incident light into three different wavelengths: 1 524 nm, 1 548 nm, and 1 572 nm. Lens #1 is constructed as a cylindrical mirror with curvature on both sides to eliminate any distortions in the system. The initial focal length of lens#1 is 90 mm before optimization. Upon passing through lens#1, the Gaussian beam undergoes compression, formatting a slender elongated spot. This

spot takes the form of a lengthy circle before optimization. After two passes through lens#1, a curved optical wedge is introduced behind it to counteract optical path length and eradicate chromatic aberration. The beam then strikes the LCoS in parallel, which is replaced by a planar reflector in simulation. Fig. 8a illustrates the layout of the optical components in simulation and the transmission paths of three beams of light of different wavelengths. The LCoS is modeled to include the mechanical structure surface, and the front and rear surfaces. The LCoS is simulated as a reflective grating, with diffractive surfaces added in different directions to represent diffraction in the x - and y -directions, as shown in Fig. 8b. To minimize the number of system optimization procedures, we initially alter the LCoS surface by rotating it at a specific angle to align with the relevant port. This allows us to adjust the rotation angle of the mirror instead of modifying the diffraction angle of the LCoS.

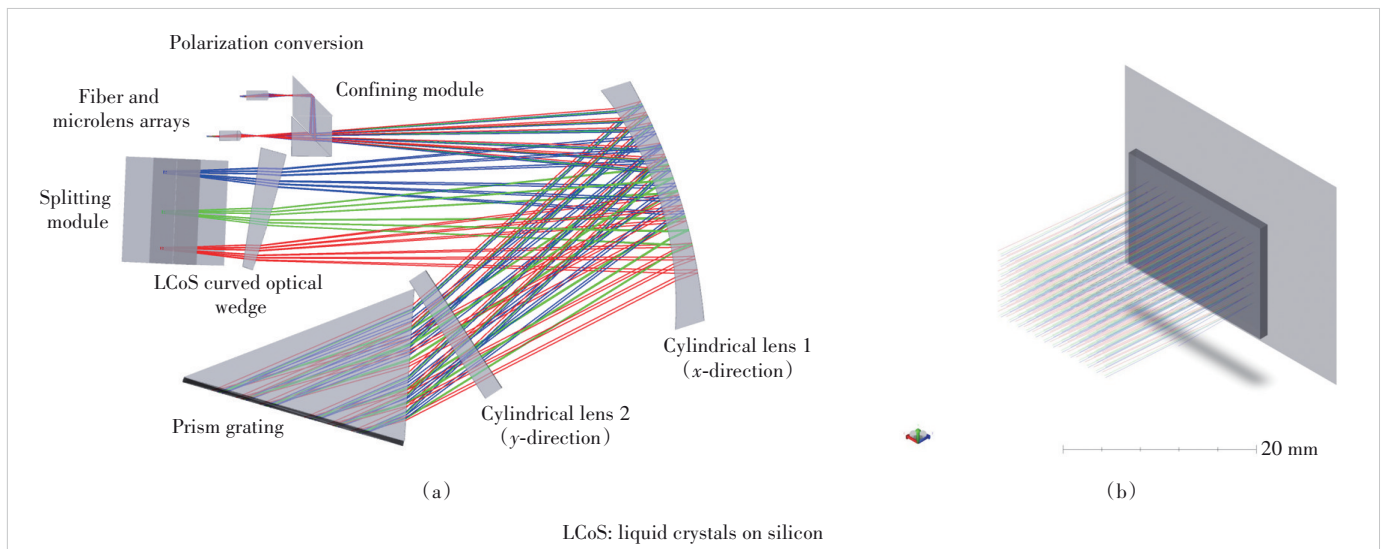
The simulation aims to achieve precise wavelength resolution while maximizing the number of ports. This is achieved by adjusting the deflection angle of the reflector, which is used to simulate the diffraction of the LCoS. Previous analysis has shown that, for the spot on the LCoS, increasing the size of its y -axis direction within the active area will result in a larger coverage of the LCoS. This would lead to more effective pixel coverage, higher diffraction efficiency, and less system transmission insertion loss. Meanwhile, the wavelength resolution can be enhanced by reducing the beam size in the x -direction of the LCoS. Eventually, to achieve the two primary goals of increasing the number of ports and improving the spectral resolution, the approach automatically optimizes the system by defining the merit function for the relevant parameters, performing iterative optimization, and utilizing the Zemax-Damped Least Squares local optimization algorithm.

The optimization of the beam incident on the LCoS is achieved by manipulating operands through the repeated modification of normalized coordinates for each wavelength within the merit function. Simultaneously, we impose restrictions on the dimensions of WSS, the width of the glass rim of the cylindrical lens, the distance between the glass layers, and the thickness of the glass. These constraints aim to prevent our gadget from undergoing significant deformation during optimization and to minimize the challenges associated with processing the component to achieve optimal results. We also adjust the optical wedge slope, the curvature of the cylindrical mirror, thickness, and air spacing to optimize the properties of the beam on the LCoS. The approach for optimizing the beam size at the exit port of the micro-lens is identical to the one used for optimizing the beam size on the LCoS. The objective is to regulate the size of the beam as it reaches the front of the micro-lens array, ensuring the beam waist size of the Gaussian beam received at the front of the micro-lens is essentially identical to that at the emitting port. This alignment guarantees improved efficiency in coupling throughout the deflection process. The merit function used in the simulation can be expressed as

$$(\text{MF})^2 = \sum_i W_i (V_i - T_i)^2 / \sum_i W_i, \quad (9)$$

where MF is the merit function, V_i is the actual value of the variable, T_i is the target value of the variable, and W_i is the weight of the variable. As mentioned before, T_i can be set as variables that affect the quality of the beams at the exit port of the micro-lens and on the LCoS. Specific variable type settings are given in Table 2.

Taking into account the symmetry of the whole optical system and optimizing for speed, our simulation establishes a to-



▲ Figure 8. Schematic diagram of the optical structure of WSS in Zemax: (a) overall component layout and (b) model of LCoS

Table 2. Target variable settings in Zemax

T_i	Variables	Operand
T_1	Coupling efficiency	POPD(0)
T_2	Beam width on LCoS	POPD(23)
T_3	Beam size of the waist near LCoS plane	POPD(7)
T_4	Overlap of beams of different polarization on LCoS	DIFF
T_5	Width of beam coverage in x -direction of LCoS	REAX
T_6	Coordinate values of different ports returning to FA	REAX
T_7	Beam size of different ports returning to FA	POPD(23)

DIFF: difference of two operands
 FA: fiber array
 LCoS: liquid crystals on silicon
 POPD: physical optics propagation data
 REAX: real ray x -coordinate

tal of 40 multi-configurations, corresponding to ports 20 to 40 of the optical system. Each port is associated with two polarization states. During the optimization process, we thoroughly assess the performance of all ports to get the most optimum system evaluation. The merit function of the system primarily assesses the coupling efficiency between each port, the extent of overlap between beams with different polarization states, the size of the beam waist on the LCoS, and the 3 dB bandwidth of the 50 GHz grid. Initially, the curvature and rotation angle of the components, as well as the distances between them, are simulated and tuned individually, which is aimed to achieve a coupling efficiency of 95% for the central wavelength returning to the central port, while also ensuring that the P-polarization and S-polarization of the beams overlap at the LCoS. Once the location and parameters of the components are confirmed, the angle and curvature of the curved optical wedge are adjusted to optimize the

coupling efficiency for the wavelengths returning to the center port, which ensures that the LCoS can cover a wavelength range from 1524 nm to 1572 nm as required. Subsequently, curved fiber arrays are adopted to compensate for the coupling mismatch caused by conic diffraction and thereby enhance the coupling effectiveness of various port switching. To improve the overall system performance, it is necessary to modify the objective and weight values based on the optimization findings, which will result in reduced merit function values. Once this optimization process is finished, the bandwidth of the proposed WSS is simulated and evaluated to determine if it satisfies the relevant requirements. This process continues until the system index is optimized to match the criteria.

4.2 Performance of Designed WSS

In this system, we primarily focus on several key aspects: system size, spot size on the LCoS, coupling efficiency of the output ports, and bandwidth performance. The overall system size is 110 mm \times 90 mm. The Gaussian beam on the LCoS, featuring 12 sampling wavelengths, is depicted in Fig. 9a. It is observed that the Gaussian beams of different wavelengths are arranged in a columnar distribution as shown in the figure, with a uniform width and centered alignment in the x -direction on the LCoS, where the spot radius is 1.015 mm and the dispersion direction spot radius is 16 μ m. Through physical optics propagation calculations in Zemax, we derived the ideal coupling efficiency for different ports, with the coupling efficiency of twins A and B ranging from 96.75% to 82.14% for almost all ports. As shown in Fig. 9b, the coupling effi-

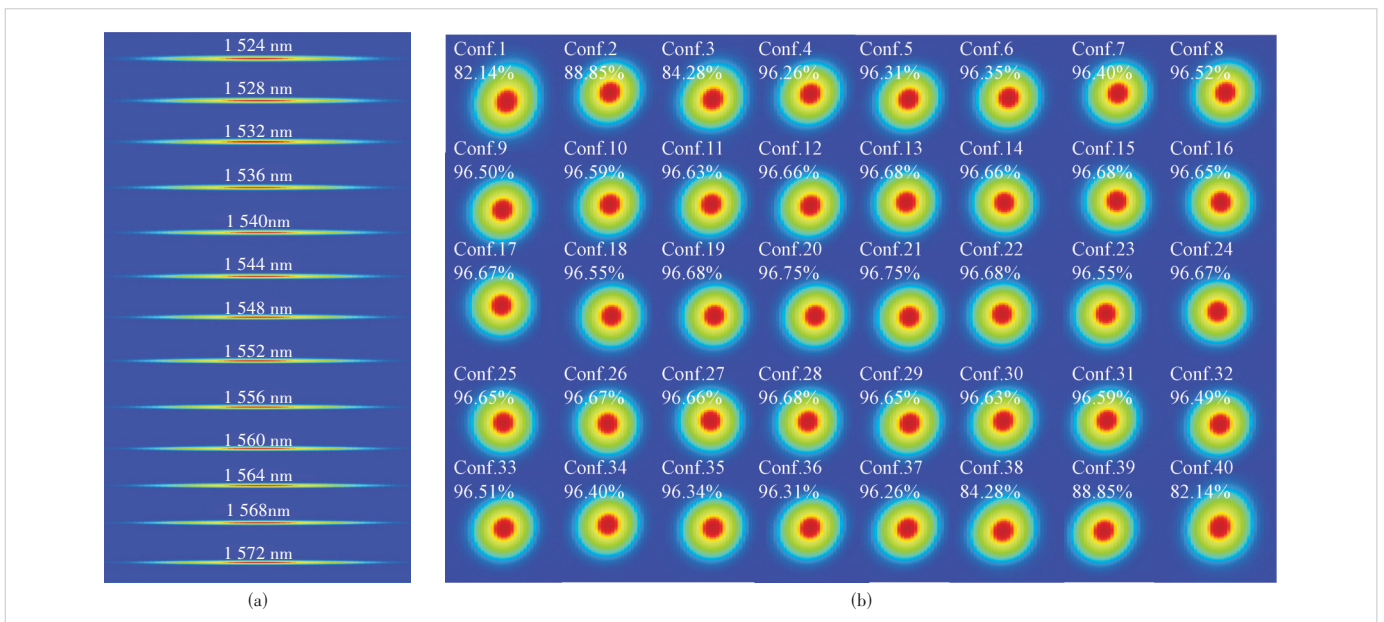


Figure 9. Deflection performance of the WSS system in Zemax: (a) layout of Gaussian beams on the LCoS and (b) shape of the beam to be coupled into the fiber

▼ **Table 3. Coupling efficiency of beam deflection for three wavelength channels and 40 ports**

Port	1 524 nm	1 550 nm	1 572 nm	Port	1 524 nm	1 550 nm	1 572 nm
1	87.00%	81.61%	60.24%	21	93.03%	96.72%	94.15%
2	91.16%	89.09%	77.83%	22	93.12%	96.65%	93.91%
3	89.42%	84.24%	87.70%	23	93.01%	96.52%	94.09%
4	91.57%	96.24%	86.84%	24	92.98%	96.65%	93.75%
5	91.80%	96.28%	90.88%	25	92.85%	96.63%	93.80%
6	92.02%	96.32%	90.82%	26	93.03%	96.65%	93.78%
7	92.07%	96.39%	91.14%	27	93.04%	96.64%	93.48%
8	92.53%	96.49%	91.60%	28	92.83%	96.65%	93.50%
9	92.36%	96.47%	92.57%	29	92.94%	96.63%	93.38%
10	92.81%	96.56%	92.54%	30	92.81%	96.60%	93.00%
11	92.81%	96.60%	93.00%	31	92.81%	96.56%	92.54%
12	92.94%	96.63%	93.38%	32	92.36%	96.47%	92.57%
13	92.83%	96.65%	93.50%	33	92.53%	96.49%	91.60%
14	93.04%	96.64%	93.48%	34	92.07%	96.39%	91.14%
15	93.03%	96.65%	93.78%	35	92.02%	96.32%	90.82%
16	92.85%	96.63%	93.80%	36	91.80%	96.28%	90.88%
17	92.98%	96.65%	93.75%	37	91.57%	96.24%	86.84%
18	93.01%	96.52%	94.09%	38	89.42%	84.24%	87.70%
19	93.12%	96.65%	93.91%	39	91.16%	89.09%	77.83%
20	93.03%	96.72%	94.15%	40	87.01%	81.61%	60.24%

ciency of twins A and B fulfills the design criteria. Table 3 illustrates the coupling efficiency of beam deflection for three wavelength channels (1 524 nm, 1 550 nm, and 1 572 nm). The coupling efficiency for beam deflection for the 1 572 nm channel experiences a notable decrease, which can be improved by further modifying the characteristics of the optical wedge and lens#1.

The bandwidths of the simulated system are also tested. By opening windows on the LCoS for long, medium, and short wavelengths, beams with a 50 GHz bandwidth are scanned at a frequency precision of 1 GHz to determine the coupling efficiency at single-frequency points. This procedure verified the 3 dB bandwidth and 0.5 dB bandwidth for the central port output. In the case of deflection of all ports, more than 44 GHz of 3 dB bandwidth can be achieved at a 50 GHz grid for all channels (120×50 GHz), as shown in Fig. 10. The theoretical calculations anticipate a 3 dB bandwidth exceeding 46 GHz. Discrepancies between this prediction and the Zemax simulations may stem from aberrations influencing the beam spot shape and the departure from an ideal 4f optical system configuration in practical implementations.

5 Conclusions

A twin 1×40 WSS is designed with theoretical analysis and simulation investigation. Polarization multiplexing is employed for the two sources of the twin WSS by polarization conversion before the common optical path. The polarization separation module realizes polarization demultiplexing before the light beam launches onto the LCoS. The parameters of prism grating are carefully designed to cover the super C band on the active area of the LCoS and obtain enough dispersion ability for fine bandwidth manipulation. The beam waist on the LCoS is carefully regulated with the micro-lens array and the lens after the birefringent crystal to guarantee optimal 3 dB bandwidth performance. The space of the fiber array is optimized to harness the isolation between the neighbor ports. Simulation results demonstrate that the coupling efficiency of our LCoS-based WSS can exceed 80%, reaching over 96% for 90% of the ports. Additionally, a 3 dB bandwidth of more than 44 GHz is obtained at a 50 GHz grid across all channels. In future studies, we will explore more ports and develop a new structure suitable for higher performance.

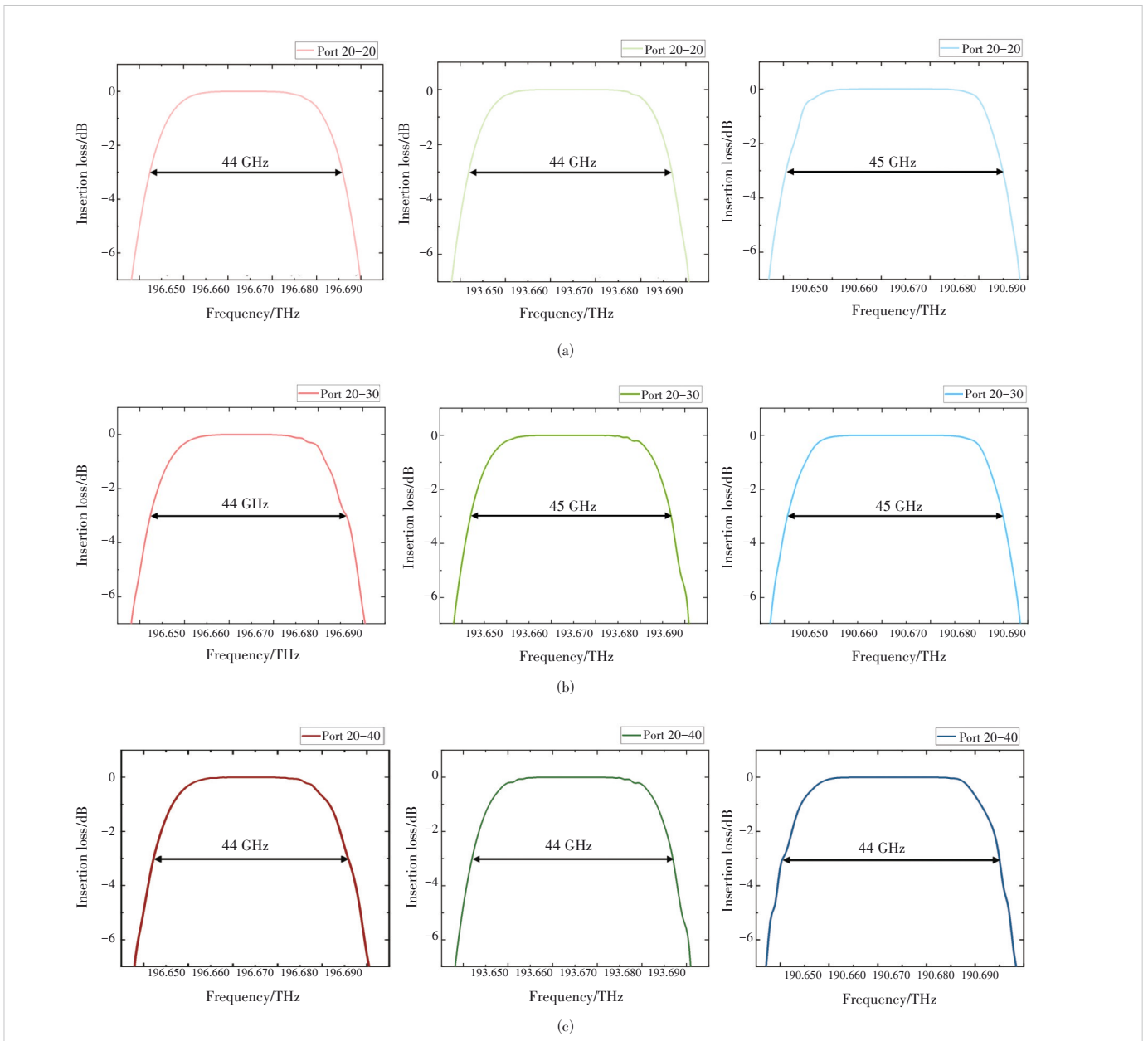
ration module realizes polarization demultiplexing before the light beam launches onto the LCoS. The parameters of prism grating are carefully designed to cover the super C band on the active area of the LCoS and obtain enough dispersion ability for fine bandwidth manipulation. The beam waist on the LCoS is carefully regulated with the micro-lens array and the lens after the birefringent crystal to guarantee optimal 3 dB bandwidth performance. The space of the fiber array is optimized to harness the isolation between the neighbor ports. Simulation results demonstrate that the coupling efficiency of our LCoS-based WSS can exceed 80%, reaching over 96% for 90% of the ports. Additionally, a 3 dB bandwidth of more than 44 GHz is obtained at a 50 GHz grid across all channels. In future studies, we will explore more ports and develop a new structure suitable for higher performance.

Acknowledgment

The authors gratefully acknowledge the support provided by ZTE Corporation for the research project on wavelength-selective switches. We are deeply indebted to Dr. YOU Quan, Ms. CHEN Wen, Mr. LI Yuzhe and Dr. LIU Chen for their unwavering support, expert guidance, and insightful discussions throughout this study. Their expertise and dedication significantly enriched the research process. We express our sincere appreciation to everyone who contributed to the success of this endeavor.

References

- [1] KOZDROWSKI S, ŻOTKIEWICZ M, SUJECKI S. Optimization of optical networks based on CDC-ROADM technology [J]. Applied sciences, 2019, 9 (3): 399. DOI: 10.3390/app9030399
- [2] FORD J E, AKSYUK V A, BISHOP D J, et al. Wavelength add-drop switching using tilting micromirrors [J]. Journal of lightwave technology, 1999, 17(5): 904 - 911. DOI: 10.1109/50.762910
- [3] DOERR C R, STULZ L W, LEVY D S, et al. Silica-waveguide 1×9 wavelength-selective cross connect [C]//Optical Fiber Communication Conference. OSA, 2002. DOI:10.1109/OFC.2002.1036752
- [4] BAXTER G, FRISKEN S, ABAKOUMOV D, et al. Highly programmable wavelength selective switch based on liquid crystal on silicon switching elements [C]//Proc. Optical Fiber Communication Conference and the National Fiber Optic Engineers Conference. IEEE, 2006. DOI: 10.1109/OFC.2006.215365
- [5] MA Y R, STEWART L, ARMSTRONG J, et al. Recent progress of wavelength selective switch [J]. Journal of lightwave technology, 2021, 39(4): 896 - 903. DOI: 10.1109/JLT.2020.3022375
- [6] HAN T, PLUMRIDGE J, FRISKEN S, et al. LCoS-based matrix switching for 2 × 4 WSS for fully flexible channel selection [C]//Proc. International Conference on Photonics in Switching (PS). IEEE, 2012: 1 - 3
- [7] YANG H N, ROBERTSON B, CHU D P. Crosstalk reduction in holographic wavelength selective switches based on phase-only LCoS devices [C]//Proc. Optical Fiber Communication Conference. OSA, 2014. DOI: 10.1364/ofc.2014.th2a.23
- [8] YANG H N, ROBERTSON B, WILKINSON P, et al. Small phase pattern 2D beam steering and a single LCOS design of 40 1 × 12 stacked wavelength selective switches [J]. Optics express, 2016, 24(11): 12240 - 12253. DOI: 10.1364/OE.24.012240
- [9] HE J, NORWOOD R A, BRANDT-PEARCE M, et al. A survey on recent



▲ Figure 10. Bandwidth performance at 50 GHz grid with the center wavelengths of 1524 nm, 1548 nm, and 1572 nm from left to right for the deflections from port 20 to 20, 30, and 40, respectively

- advances in optical communications [J]. *Computers & electrical engineering*, 2014, 40(1): 216 - 240. DOI: 10.1016/j.compeleceng.2013.11.017
- [10] ROBERTSON B, YANG H N, REDMOND M M, et al. Demonstration of multi-casting in a 1×9 LCoS wavelength selective switch [J]. *Journal of lightwave technology*, 2014, 32(3): 402 - 410. DOI: 10.1109/JLT.2013.2293919
- [11] WANG M, ZONG L J, MAO L, et al. LCoS SLM study and its application in wavelength selective switch [J]. *Photonics*, 2017, 4(2): 22. DOI: 10.3390/photonics4020022
- [12] MILEWSKI G, ENGSTRÖM D, BENGTTSSON J. Diffractive optical elements designed for highly precise far-field generation in the presence of artifacts typical for pixelated spatial light modulators [J]. *Applied optics*, 2007, 46(1): 95 - 105. DOI: 10.1364/AO.46.000095
- [13] PERSSON M, ENGSTRÖM D, BENGTTSSON J, et al. Realistic treatment of spatial light modulator pixelation in real-time design algorithms for holographic spot generation [C]//Proc. Digital Holography and Three-Dimensional Imaging. OSA, 2011. DOI: 10.1364/dh.2011.dwc32
- [14] PERSSON M, ENGSTRÖM D, GOKSÖR M. Reducing the effect of pixel crosstalk in phase only spatial light modulators [J]. *Optics express*, 2012, 20(20): 22334 - 22343. DOI: 10.1364/OE.20.022334
- [15] NIE J W, DONG L Y, TONG X W, et al. Phase flicker minimisation for crosstalk suppression in optical switches based on digital liquid crystal on silicon devices [J]. *Optics express*, 2021, 29(7): 10556 - 10567. DOI: 10.1364/OE.415800
- [16] ROBERTSON B, ZHANG Z C, YANG H N, et al. Reduction of crosstalk in a colourless multicasting LCOS-based wavelength selective switch by

the application of wavefront encoding [C]//Proc. Next-Generation Optical Communication: Components, Sub-Systems, and Systems. SPIE, 2012. DOI: 10.1117/12.907281

- [17] HUANG L H., RAO C H. Wavefront sensorless adaptive optics: a general model-based approach [J]. Optics express, 2011, 19(1): 371 - 379. DOI: 10.1364/OE.19.000371
- [18] FRISKEN S J. Polarization diverse wavelength selective switch: US20170214482 [P]. 2017
- [19] ZHOU Y R, KEENS J, WAKIM W. High capacity innovations enabling scalable optical transmission networks [J]. Journal of lightwave technology, 2023, 41(3): 957 - 967. DOI: 10.1109/JLT.2022.3206277
- [20] MAROM D M, NEILSON D T, GREYWALL D S, et al. Wavelength-selective $1 \times K$ switches using free-space optics and MEMS micromirrors: theory, design, and implementation [J]. Journal of lightwave technology, 2005, 23(4): 1620 - 1630. DOI: 10.1109/JLT.2005.844213

Biographies

WANG Han received her BS degree from Beijing Jiaotong University, China and is pursuing a master's degree at Huazhong University of Science and Technology, China. Her research interests include the optical design of wavelength selective switches and LCoS algorithms, with a current focus on designing multi-band integrated WSS and $M \times N$ WSS.

LIU Maoqi received his bachelor's degree from the School of Optical and Electronic Information, Huazhong University of Science and Technology, China. Currently, he is a joint PhD student at the National Engineering Laboratory for Next Generation Internet Access System, Huazhong University of Science and Technology, and the Photonics Research Institute, Hong Kong Polytechnic University, China. His research primarily focuses on multi-band WSS, aiming to improve their efficiency and scalability in modern optical networks. Additionally, he explores the integration of optical fiber communication and sensing, seeking innovative solutions to combining these technologies for multifunctional applications in 6G telecommunications.

FENG Zhenhua received his PhD from Huazhong University of Science and Technology, China in 2017. He has been engaged in the research and development of optical fiber communication systems and algorithms for about five years with more than 70 journal and conference publications and about 10 granted patents. His research interests mainly lie in the design and verification of optical transmission systems and DSP algorithms.

LIU Minghuan received his PhD from Changchun Institute of Optics, Fine Mechanics and Physics, Chinese Academy of Sciences. He has worked in the Wavelength Division System Department of the Cable Research Institute, ZTE Corporation since June 2023, engaged in the work related to WSS design.

MAO Baiwei (mao.baiwei@zte.com.cn) received his PhD from Nankai University, China in 2022. He has worked in the Wavelength Division System Department of the Cable Research Institute, ZTE Corporation since July 2022, engaged in optical transmission system planning and optimization.